

# Exclusive $\gamma^{(*)}\gamma$ processes

V.L. Chernyak<sup>1)</sup>

Budker Institute of Nuclear Physics, 630090 Novosibirsk, Russia

**Abstract** A short review of experimental and theoretical results on the large angle cross sections “ $\gamma\gamma \rightarrow$  two mesons” and the form factors  $\gamma^*\gamma \rightarrow P = \{\pi, \eta, \eta'\}$  is given.

**Key words** mesons, two photon processes, form factor

**PACS** 12.39.-x, 13.40.-f, 13.60.Le

## 1 Introduction

The general approach to calculations of hard exclusive processes in QCD was developed in [1, 2]. In particular, the general formula for the leading power term of any hadron form factor  $\gamma^* \rightarrow H_1 H_2$  has the form [1]:

$$\langle p_1, s_1, \lambda_1; p_2, s_2, \lambda_2 | J_\lambda | 0 \rangle = C_{12} \left( 1/\sqrt{q^2} \right)^{|\lambda_1 + \lambda_2| + (2n_{\min} - 3)}, \quad (1)$$

where:  $n_{\min}$  is the minimal number of elementary constituents in a given hadron,  $n_{\min} = 2$  for mesons and  $n_{\min} = 3$  for baryons;  $s_{1,2}$  and  $\lambda_{1,2}$  are the hadron spins and helicities, the current helicity  $\lambda = \lambda_1 - \lambda_2 = 0, \pm 1$ ; the coefficient  $C_{12}$  is expressed through the integral over the wave functions of both hadrons.

It is seen that the behavior is independent of hadron spins, but depends essentially on their helicities, and the QCD helicity selection rules are clearly seen: the largest form factors occur only for  $\lambda_1 = \lambda_2 = 0$  mesons and  $\lambda_1 = -\lambda_2 = \pm 1/2$  baryons of any spins.

The QCD logarithmic loop corrections to (1) were first calculated in [2] (see also [3–5], for a review

see [6]).

## 2 $\gamma\gamma \rightarrow \bar{M}M$ large angle scattering

The QCD predictions for the leading terms of the large angle scattering cross sections  $\gamma\gamma \rightarrow$  two mesons were considered in [7, 8] (see also [9] for the one-loop corrections).

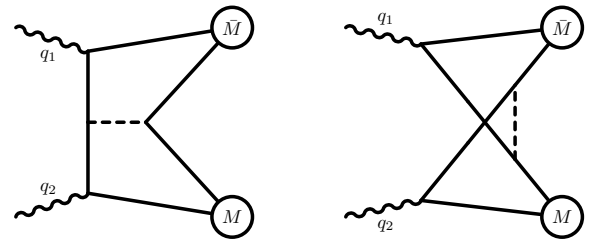


Fig. 1. Two typical lowest order Feynman diagrams for the leading term hard QCD contributions to  $\gamma\gamma \rightarrow \bar{M}M$ , the broken line is the hard gluon exchange.

The expressions for the cross sections look as (the example in (2) is given for  $\gamma\gamma \rightarrow K^+K^-$ ):

$$\begin{aligned} \frac{d\sigma(\gamma\gamma \rightarrow M^\dagger M)}{d\cos\theta} &= \frac{1}{32\pi W^2} \frac{1}{4} \sum_{\lambda_1 \lambda_2} |A_{\lambda_1 \lambda_2}|^2, \\ A_{\lambda_1 \lambda_2}^{(\text{lead})}(W, \theta) &= \frac{64\pi^2}{9W^2} \alpha \bar{\alpha}_s f_P^2 \int_0^1 dx \phi_P(x) \int_0^1 dy \phi_P(y) T_{\lambda_1 \lambda_2}(x, y, \theta), \\ T_{++} = T_{--} &= (e_u - e_s)^2 \frac{1}{\sin^2\theta} \frac{A}{D}, \\ T_{+-} = T_{-+} &= \frac{1}{D} \left[ \frac{(e_u - e_s)^2}{\sin^2\theta} (1 - A) + e_u e_s \frac{AC}{A^2 - B^2 \cos^2\theta} + \frac{(e_u^2 - e_s^2)}{2} (x_u - y_s) \right], \end{aligned} \quad (2)$$

Received 26 January 2010

1) E-mail: v.l.chernyak@inp.nsk.su

©2009 Chinese Physical Society and the Institute of High Energy Physics of the Chinese Academy of Sciences and the Institute of Modern Physics of the Chinese Academy of Sciences and IOP Publishing Ltd

$$A = (x_s y_u + x_u y_s), \quad B = (x_s y_u - x_u y_s),$$

$$C = (x_s x_u + y_s y_u), \quad D = x_u x_s y_u y_s,$$

where:  $x_s + x_u = 1$ ,  $e_u = 2/3$ ,  $e_s = e_d = -1/3$ ,  $f_P$  are the couplings:  $f_\pi \simeq 132$  MeV,  $f_K \simeq 162$  MeV,  $\phi_P(x)$  is the leading twist pseudoscalar meson wave function (= distribution amplitude), “ $x$ ” is the meson momentum fraction carried by quark inside the meson.

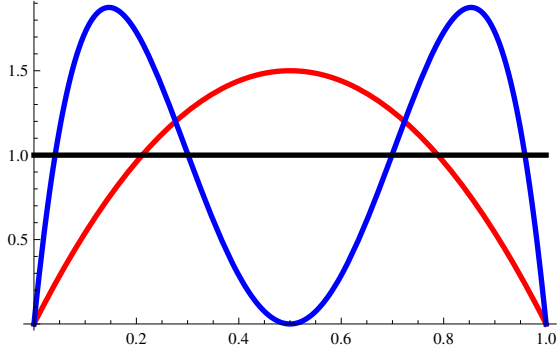


Fig. 2. Three different models for the leading twist pion wave function  $\phi_\pi(x)$ . Red line - asymptotic wave function  $\phi_\pi^{\text{asy}}(x) = 6x(1-x)$ . Blue line - CZ wave function (at the low scale normalization point  $\mu \sim 1$  GeV):  $\phi_\pi^{\text{cz}}(x) = 30x(1-x)(2x-1)^2$  [10]. Black line - flat wave function  $\phi_\pi(x) = 1$ .

Cross sections for charged mesons:  $\gamma\gamma \rightarrow \pi^+\pi^-, K^+K^-$  behave as:

$$\frac{d\sigma(\gamma\gamma \rightarrow \pi^+\pi^-)}{d\cos\theta} \sim \frac{f_\pi^4}{W^6 \sin^4\theta}, \quad (3)$$

and the angular distribution  $\sim 1/\sin^4\theta$  is only weakly dependent of the meson wave function form. But the absolute values of cross sections depend strongly on the form of  $\phi_M(x)$  and are much larger for the wide wave functions.

For neutral mesons:  $\gamma\gamma \rightarrow \pi^0\pi^0, \bar{K}_S K_S, \pi^0\eta, \eta\eta$  the coefficient of the formally leading term  $\sim 1/W^6$  is very small, so that at present energies  $W < 4$  GeV such amplitudes are dominated by the first power correction in the amplitude and the energy behavior is much steeper:

$$\frac{d\sigma(\gamma\gamma \rightarrow \bar{K}_S K_S)}{d\cos\theta} \sim \frac{f_K^4}{W^{10}} \chi(\theta), \quad (4)$$

1) It was “obtained” in [11] that the angular behavior of the standard handbag contribution from Fig. 3(a) is  $d\sigma/d\cos\theta \sim 1/\sin^4\theta$ . Really, this “result” is completely model dependent. The reason is that a number of special approximate relations were used in [11] at intermediate steps. All these relations are valid, at best, for the leading term only. But it turned out finally that their would be leading term gives zero contribution to the amplitude, and the whole answer is due to next corrections, which were not under control in [11]. Their result  $\sim 1/\sin^4\theta$  is completely due to especially (and arbitrary) chosen form of the next to leading correction, while ignoring all others next to leading corrections of the same order of smallness. Therefore, there is no really model independent prediction of the angular dependence in [11]. So, it is not surprising that the explicit calculation in [12] give different angular dependence.

while, unlike (3), the angular dependence  $\chi(\theta)$  and the overall coefficient in (4) are not predicted (at present) in a model independent way.

As the alternative approach to description of  $\gamma\gamma \rightarrow \bar{M}M$  processes, the “handbag model” was used in [11]. The main dynamical assumption of the “handbag model” [11] is that at present energies  $W \leq 4$  GeV all  $\gamma\gamma \rightarrow \bar{M}M$  amplitudes are still dominated by soft non-leading terms.

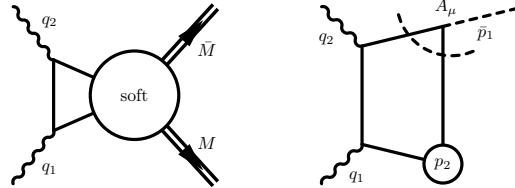


Fig. 3. (a) The overall picture of the “standard handbag” contribution [11]. (b) The standard lowest order Feynman diagram for the QCD light cone sum rule [12].

For all mesons, both charged and neutral, “the standard handbag” contribution (Fig. 3) gives:  $d\sigma(\gamma\gamma \rightarrow \bar{M}M)/d\cos\theta \sim \text{const}/W^{10}$  [12]. This angular behavior  $\sim \text{const}$  disagrees with all data  $\sim 1/\sin^4\theta$ , and the energy behavior disagrees with the data  $\sim 1/W^6$  for charged mesons<sup>1)</sup>.

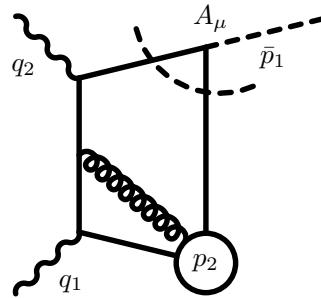


Fig. 4. The typical additional Feynman diagram for the “extended handbag model” which includes contributions from 3-particle wave functions (the curly line is the near mass shell non-perturbative gluon).

I expect that, in distinction with the standard contribution of Fig. 3, such additional contributions

will give

$$\left(\frac{d\sigma(\gamma\gamma \rightarrow \bar{M}M)}{d\cos\theta}\right)_{\text{fig.3}} \sim \frac{1}{W^{10}},$$

$$\left(\frac{d\sigma(\gamma\gamma \rightarrow \bar{M}M)}{d\cos\theta}\right)_{\text{fig.4}} \sim \frac{1}{W^{10}\sin^4\theta}, \quad (5)$$

in better agreement with data for neutral mesons  $M = \pi^0, K_S, \eta$ . Unfortunately, such contributions are not yet calculated at present (and it well may be that they are too small in absolute values).

Now, about a comparison with the data. The Belle results for  $\gamma\gamma \rightarrow \pi^+\pi^-$  and  $\gamma\gamma \rightarrow K^+K^-$  [14] are presented in Fig. 5<sup>1)</sup>.

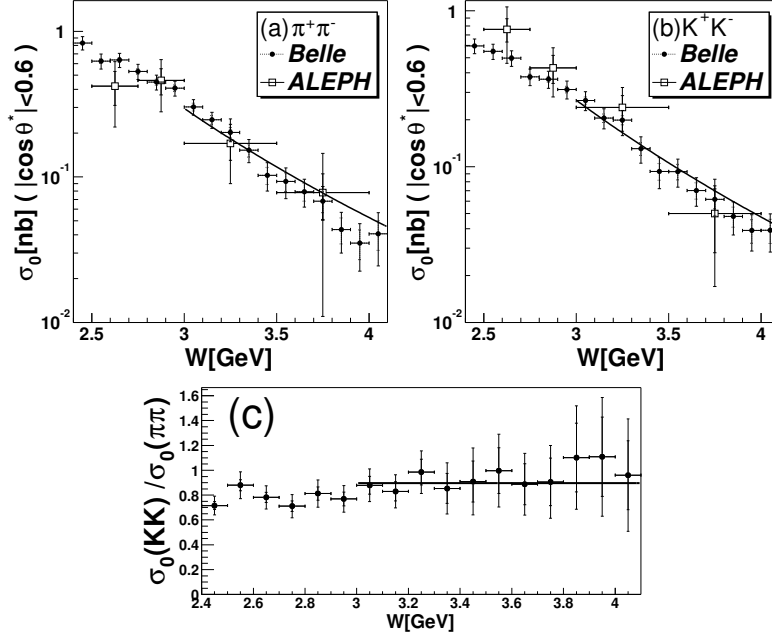


Fig. 5. (a), (b) Cross sections  $\sigma_0$  integrated over the angular region  $|\cos\theta| < 0.6$ , together with the  $\sim (1/W)^6$  dependence line [14]. (c) the cross section ratio  $R_{\text{exp}} = \sigma_0(KK)/\sigma_0(\pi\pi) \simeq 0.9$  [14]. Compare  $R_{\text{exp}}$  with the naive prediction  $R = (f_K/f_\pi)^4 \simeq 2.3$ .

It is seen that they are compatible with the leading term QCD predictions  $\sigma(\pi^+\pi^-) \sim \sigma(K^+K^-) \sim 1/W^6$ , and disagree with the handbag model predictions of much steeper behavior  $\sim 1/W^{10}$ . The angular behavior measured by Belle [14] for  $\pi^+\pi^-$  and  $K^+K^-$  is  $\sim 1/\sin^4\theta$ , also in agreement with QCD and in disagreement with the standard handbag model [12]. As for the absolute values of cross sections, for the pion (kaon) wave functions close to  $\phi_{\text{asy}}(x)$  the predicted from (2) cross sections are much smaller than data, while predictions from (2) for the wide  $\pi$  and  $K$  wave functions like  $\phi_{\text{cz}}(x)$  are in a reasonable agreement with data (see [12] for more detail).

Now, let us compare with the Belle results for the neutral mesons. The results for the cross section  $\gamma\gamma \rightarrow K_S K_S$  are published in [15], see Fig. 6.

It is seen from Fig. 6 that in the energy range  $2.5 < W < 4$  GeV the energy behavior  $\sim 1/W^{10}$  in this

neutral channel is much steeper in comparison with  $\sim 1/W^6$  in the charged channel. This agrees with qualitative expectations from QCD that because the coefficient of the formally leading at sufficiently large  $W$  is very small, the first non-leading term dominates the  $K_S K_S$ -amplitude at present energies  $W < 4$  GeV. Let us recall that the handbag model predicts the dominance of non-leading terms (and so the energy behavior  $\sim 1/W^{10}$ ) for all mesons, both charged and neutral.

As for the angular distribution, the data are sufficiently well described by  $\sim 1/\sin^4\theta$  [15]. Let us recall once more that “the standard handbag model” (Fig. 3) predicts the flat angular distribution  $\sim \text{const}$  [12] also for all mesons, but the qualitative expectation is that “the extended handbag model” (Fig. 4) will give  $\sim 1/\sin^4\theta$ , see (5).

1) The reason for  $R_{\text{exp}} \ll (f_K/f_\pi)^4$  is that the leading twist pseudoscalar meson wave function  $\phi_P(x)$  becomes narrower when the lighter u or d quarks are replaced with the heavier s quarks, and this opposite effect compensates those from  $f_K/f_\pi > 1$ , see [8].

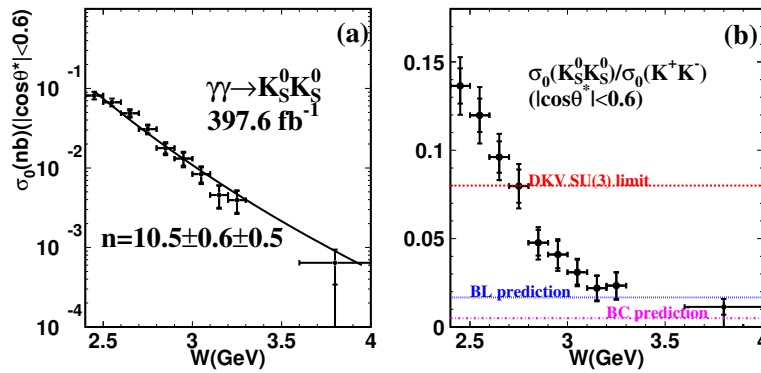


Fig. 6. (a) The total cross section  $\sigma_0(\gamma\gamma \rightarrow K_S K_S)$  in the c.m. angular region  $|\cos\theta^*| < 0.6$  [15]. Here  $n$  is the  $W$ -dependence  $\sigma_0(W) \sim W^{-n}$ ; (b) The ratio  $\sigma_0(K_S K_S)/\sigma_0(K^+ K^-)$  versus  $W$ . The dotted line DKV = Diehl-Kroll-Vogt is the handbag model prediction with the  $SU(3)$ -flavor symmetry assumption [11]; the dashed BL line is the Brodsky-Lepage [7] prediction for the kaon wave function close to  $\phi_{\text{asy}}(x)$ , the dashed-dotted BC line is the Benayoun-Chernyak [8] prediction for the kaon wave function like  $\phi_{\text{cz}}(x)$  (both are the leading term QCD predictions (2) for sufficiently large energy  $W$ ).

Table 1. The value of “ $n$ ” in  $\sigma_{\text{tot}} \sim (1/W)^n$  in various reactions fitted in the  $W$  and  $|\cos\theta|$  ranges indicated.

process	$n$ -experiment	$W$ range/GeV	$ \cos\theta $	Ref.	$n$ -QCD	$n$ -handbag
$\pi^+ \pi^-$	$7.9 \pm 0.4_{\text{stat}} \pm 1.5_{\text{syst}}$	3.0–4.1	$< 0.6$	[14]	$\simeq 6$	$\simeq 10$
$K^+ K^-$	$7.3 \pm 0.3_{\text{stat}} \pm 1.5_{\text{syst}}$	3.0–4.1	$< 0.6$	[14]	$\simeq 6$	$\simeq 10$
$K_S^0 K_S^0$	$10.5 \pm 0.6_{\text{stat}} \pm 0.5_{\text{syst}}$	2.4–4.0	$< 0.6$	[15]	$\simeq 10$	$\simeq 10$
$\eta \pi^0$	$10.5 \pm 1.2_{\text{stat}} \pm 0.5_{\text{syst}}$	3.1–4.1	$< 0.8$	[17]	$\simeq 10$	$\simeq 10$
$\pi^0 \pi^0$	$8.0 \pm 0.5_{\text{stat}} \pm 0.4_{\text{syst}}?$	3.1–4.1	$< 0.8$	[16]	$\simeq 10$	$\simeq 10$

Finally, about the ratio  $R = \sigma_0(K_S K_S)/\sigma_0(K^+ K^-)$ , see Fig. 6(b). In the  $SU(3)$  flavor symmetry limit the standard (and extended) handbag model predicts  $R = 0.08$  [11]. It is seen from Fig. 6(b) that this ratio decreases rapidly with energy and becomes smaller than  $\sim 0.08$  at  $W > 2.7$  GeV, in disagreement with the handbag model. This is because the energy dependence of  $\sigma_0(K^+ K^-) \sim 1/W^6$  disagrees with the handbag model prediction  $\sim 1/W^{10}$ .

The QCD prediction is that at sufficiently large  $W$ , when the parametrically leading but having a small coefficient term will become dominant in the  $K_S K_S$  amplitude, this ratio will become constant (see BL and BC lines in Fig. 6(b)). It is seen from Fig. 6(b) that the ratio  $R$  is already close to the leading term QCD predictions for  $K_S K_S$  at  $W \simeq 4$  GeV.

The qualitative situation with other neutral modes,  $\gamma\gamma \rightarrow \pi^0 \pi^0, \pi^0 \eta, \eta \eta, \eta \eta'$ , etc., is similar to those of  $\gamma\gamma \rightarrow K_S K_S$ . Recently, there appeared new data from the Belle Collaboration on cross sections  $\gamma\gamma \rightarrow \pi^0 \pi^0$  and  $\gamma\gamma \rightarrow \pi^0 \eta$  [16, 17], see Figs. 7, 8 and Table 1. The QCD predictions for this range of energies are:  $\sigma(\pi^+ \pi^-) \sim 1/W^6$ ,  $\sigma(\pi^0 \pi^0) \sim \sigma(\pi^0 \eta) \sim 1/W^{10}$ ,  $R = \sigma(\pi^0 \pi^0)/\sigma(\pi^+ \pi^-) \sim 1/W^4$ . The handbag model prediction is:  $R = \sigma(\pi^0 \pi^0)/\sigma(\pi^+ \pi^-) = 1/2$ . As

for the cross section  $\sigma(\gamma\gamma \rightarrow \pi^0 \eta)$ , it behaves “normally”,  $\sim 1/W^{10}$ , similarly to  $\sigma(\gamma\gamma \rightarrow K_S K_S)$ , see Fig. 8(a). But as for  $\sigma(\gamma\gamma \rightarrow \pi^0 \pi^0)$ , it behaves “abnormally”, see Fig. 7. This last behavior agrees neither with QCD, nor with the handbag model.

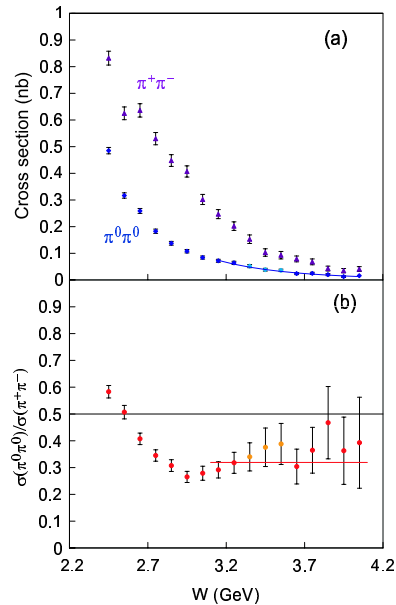


Fig. 7. (a) Cross sections  $\sigma_0(\gamma\gamma \rightarrow \pi^0 \pi^0)$  and  $\sigma_0(\gamma\gamma \rightarrow \pi^+ \pi^-)$  for  $|\cos\theta^*| < 0.6$  [14, 16]; (b) Their ratio.

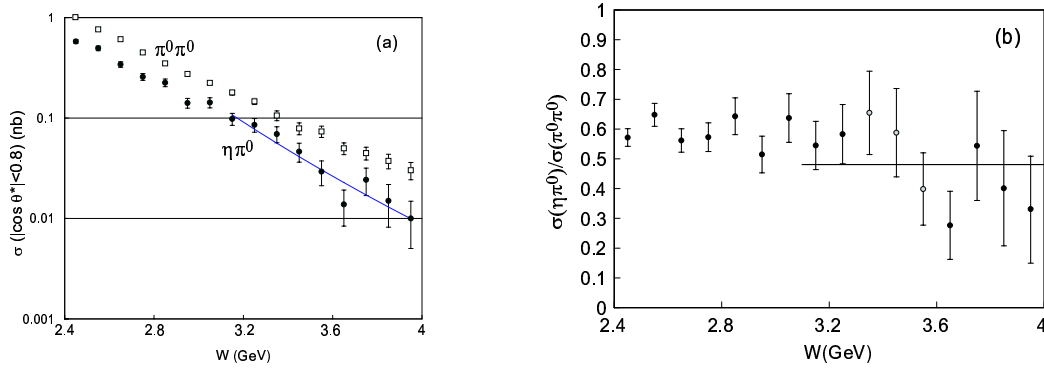


Fig. 8. (a)  $W$  - dependence of cross sections  $\gamma\gamma \rightarrow \pi^0\pi^0$  and  $\gamma\gamma \rightarrow \pi^0\eta$  ( $|\cos\theta^*| < 0.8$ ) [16, 17]. The curve is the fit:  $\sigma(\pi^0\eta) \sim W^{-n}$ ,  $n = (10.5 \pm 1.2 \pm 0.5)$ . (b)  $W$  - dependence of the cross section ratio  $\sigma(\eta\pi^0)/\sigma(\pi^0\pi^0)$  ( $|\cos\theta^*| < 0.8$ ).

### 3 Conclusions on the large angle cross sections $\gamma\gamma \rightarrow \overline{M}M$

1) The leading term QCD predictions  $d\sigma/d\cos\theta \sim 1/(W^6 \sin^4\theta)$  for charged mesons  $\pi^+\pi^-$ ,  $K^+K^-$  agree with data both in energy and angular dependence at energies  $W \gtrsim 3$  GeV. The absolute values of cross sections are in a reasonable agreement with data only for the wide  $\pi$  (K) wave functions like  $\phi_{\pi,K}^{cz}(x)$ , the asymptotic wave functions  $\phi_{\pi,K}(x) \simeq \phi^{\text{asy}}(x)$  predict much smaller cross sections (see [8, 12] for more detail). The handbag model predictions for charged mesons disagree with data in energy dependence.

2) For neutral mesons the QCD leading terms have much smaller overall coefficients, so that the non-leading terms are expected to dominate at present energies and the energy dependence is steeper:  $\sigma(\overline{M}^0M^0) \sim 1/W^{10}$ . This agrees with data on  $\sigma(\overline{K}_S K_S)$  and  $\sigma(\pi^0\eta)$ , while  $\sigma(\pi^0\pi^0)$  behaves “abnormally” (may be due to contamination of data with the pure QED - background).

3) Predictions of the “standard handbag model” disagree with data either in energy and/or angular dependence, or in absolute values. However, it is not excluded that adding soft contributions from the 3-particle wave functions in the “extended handbag model” (see Fig. 4) can help to describe cross sections of neutral mesons at intermediate energies  $2.5 \text{ GeV} < W < 4$ . Unfortunately, such contributions are not yet calculated at present (and it well may be that they are too small; besides, one has to remember that there are also power corrections due to the higher twist wave function components in the diagrams in Fig. 1).

### 4 $\gamma^*\gamma \rightarrow P = \{\pi^0, \eta, \eta'\}$ form factors $F_{\gamma P}(Q^2)$

As was first obtained in [2] on the example of the pion form factor  $F_\pi(Q^2)$  (see [3] for more details), the contributions from short and large distances factorize in  $F_\pi(Q^2)$  at large  $Q^2$ , and the logarithmic evolution of  $Q^2 F_\pi(Q^2)$  is determined by renormalization factors of operators with the same anomalous dimensions  $\gamma_n$  as in the deep inelastic scattering. So, the strict QCD prediction for  $F_\pi(Q^2)$  looks as ( $b_0 = 11 - 2n_f/3$ ,  $\mu_0 \sim 1$  GeV):

$$F_\pi(Q^2) \rightarrow \frac{8\pi\alpha_s(Q^2)|f_\pi|^2}{Q^2} \left( 1 + O\left(\frac{\alpha_s(Q)}{\alpha_s(\mu_0)}\right)^{\frac{50}{9b_0}} \right) = \frac{32\pi^2|f_\pi|^2}{b_0 Q^2 \ln Q^2} \left( 1 + O\left(\frac{\alpha_s(Q)}{\alpha_s(\mu_0)}\right)^{\frac{50}{9b_0}} \right).$$

This corresponds to the pion wave function  $\phi_\pi(x, \mu \rightarrow \infty)$  evolving to its universal asymptotic form

$$\phi_\pi(x, \mu \gg 1 \text{ GeV}) \rightarrow 6x(1-x) \left( 1 + O\left(\frac{\alpha_s(\mu)}{\alpha_s(\mu_0)}\right)^{\frac{50}{9b_0}} \right),$$

independently of its form  $\phi_\pi(x, \mu_0 \sim 1 \text{ GeV})$  at low energy. As it is seen, the logarithmic evolution with increasing scale is very slow.

As for the form factor  $F_{\gamma\pi}(Q^2) = F_{\gamma\pi}(Q^2 = -q_1^2, q_2^2 = 0)$ , the QCD prediction<sup>1)</sup> for its asymptotic behavior looks as (see e.g. [5]):

$$\int dz e^{iq_1 z} \langle \pi(p) | T \{ J_\mu(z) J_\nu(0) \} | 0 \rangle = (i\epsilon_{\mu\nu\lambda\sigma} q_1^\lambda q_2^\sigma) F_{\gamma\pi}(Q^2),$$

1) Really, unlike  $F_\pi(Q^2)$ , the asymptotic behavior of  $F_{\gamma\pi}(Q^2)$  can be directly obtained from the standard Wilson operator expansion of  $J_\mu(z)J_\nu(0)$  in (6) [18], as in calculations of the deep inelastic scattering.

$$Q^2 F_{\gamma\pi}(Q^2) = \frac{\sqrt{2}f_\pi}{3} \int_0^1 dx \frac{\phi_\pi(x, \mu \sim Q)}{x} \left( 1 + O(\alpha_s(Q)) \right) = \sqrt{2}f_\pi \left( 1 + O\left(\frac{\alpha_s(Q)}{\alpha_s(\mu_0)}\right)^{\frac{50}{9b_0}} + O(\alpha_s(Q)) \right). \quad (6)$$

For the  $\eta$  and  $\eta'$  mesons, the form factors  $F_{\gamma\eta}$  and  $F_{\gamma\eta'}$  look similarly to  $F_{\gamma\pi}$ . For instance, a simplified description of  $|\eta\rangle, |\eta'\rangle$  states in the quark flavor basis looks as follows [19]:

$$\begin{aligned} |\pi^0\rangle &\rightarrow |(\bar{u}u - \bar{d}d)/\sqrt{2}\rangle, |n\rangle \rightarrow |(\bar{u}u + \bar{d}d)/\sqrt{2}\rangle, \\ &|s\rangle \rightarrow |\bar{s}s\rangle, \\ |\eta\rangle &= \cos\phi|n\rangle - \sin\phi|s\rangle, |\eta'\rangle = \sin\phi|n\rangle + \cos\phi|s\rangle. \\ f_\pi &\simeq 132 \text{ MeV}, \quad f_n \simeq f_\pi, \quad f_s \simeq 1.3f_\pi, \quad \phi \simeq 38^\circ. \end{aligned} \quad (7)$$

$$F_{\gamma\pi}(Q^2) = \frac{\sqrt{2}(e_u^2 - e_d^2)f_\pi}{Q^2} \int_0^1 dx \frac{\phi_\pi(x, \mu \sim Q)}{x} I_0,$$

$$F_{\gamma n}(Q^2) = \frac{\sqrt{2}(e_u^2 + e_d^2)f_\pi}{Q^2} \int_0^1 dx \frac{\phi_\pi(x, \mu \sim Q)}{x} I_0,$$

$$F_{\gamma s}(Q^2) = \frac{2e_s^2 f_s}{Q^2} \int_0^1 dx \frac{\phi_s(x, \mu \sim Q)}{x} I_0,$$

$$F_{\gamma\eta}(Q^2) = \left( \cos\phi F_{\gamma n}(Q^2) - \sin\phi F_{\gamma s}(Q^2) \right),$$

$$F_{\gamma\eta'}(Q^2) = \left( \sin\phi F_{\gamma n}(Q^2) + \cos\phi F_{\gamma s}(Q^2) \right). \quad (8)$$

Predictions for  $F_{\gamma\pi}(Q^2)$  were given in a large number of theoretical papers, using many different models for the leading twist pion wave function  $\phi_\pi(x, \mu)$ . The previous data for  $F_{\gamma\pi}(Q^2)$  [20, 21] covered the space-like region  $0 < Q^2 < 8 \text{ GeV}^2$ . The recent data from BABAR [23, 24] extended this one to  $Q^2 \lesssim 40 \text{ GeV}^2$ , see Fig. 9. It is seen that  $Q^2 F_{\gamma\pi}(Q^2)$  exceeds its asymptotic value  $\sqrt{2}f_\pi$  (the dashed line in Fig.9) at  $Q^2 \gtrsim 10 \text{ GeV}^2$ . Because the loop and leading power corrections are negative here, this shows that the leading twist pion wave function  $\phi_\pi(x, \mu)$  is considerably wider than  $\phi_{\text{asy}}(x)$ , while most theoretical models predicted  $\phi_\pi(x, \mu) \simeq \phi_{\text{asy}}(x)$ . The red curve in Fig. 9 shows that, with power corrections of reasonable size, the wide leading twist pion wave function

$\phi_{cz}(x, \mu)$  obtained in [10] using the standard QCD sum rules, see Fig. 2, is not in contradiction with data<sup>1)</sup>.

Theory of the form factor  $\Phi \equiv Q^2 F_{\gamma\pi}(Q^2)$ : a) logarithmic loop corrections are calculated (in part) at the NNLO [29, 30]; b) only the part of the total power correction  $\sim 1/Q^2$  is calculated at present in [31],  $\delta\Phi_4 \simeq -\sqrt{2}f_\pi(0.6 \text{ GeV}^2)/Q^2$ , originating from the 2- and 3- particle pion wave functions of twist 4 [32] (and it well may be that it is not even the main part of the total  $\sim 1/Q^2$  correction, as there are also the contributions  $\sim 1/Q^2$  from the 4- particle wave functions of twist 4 and, moreover, the twist expansion breaks down at this level, so that the higher twist  $\geq 6$  terms also give contributions  $\sim 1/Q^2$ ); c) the power correction  $\sim 1/Q^4$  is unknown.

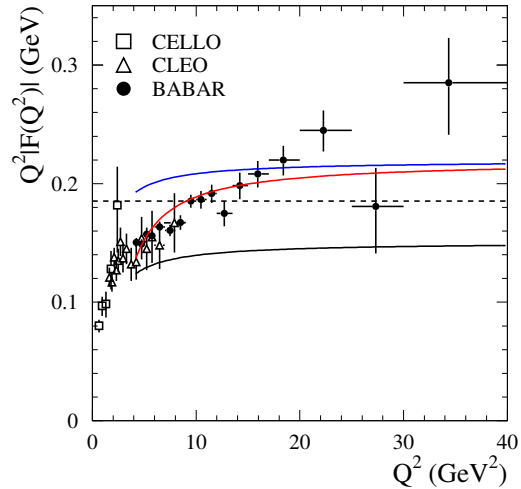


Fig. 9. Black line:  $\phi_\pi(x) = \phi_{\text{asy}}(x)$ ,  $\Phi \simeq \sqrt{2}f_\pi \left[ 0.77 - (0.6 \text{ GeV}^2/Q^2) \right]$  [29–31]. Blue line:  $\phi_\pi(x) = \phi_{cz}(x)$ ,  $\Phi \simeq \sqrt{2}f_\pi \left[ 1.18 - (0.6 \text{ GeV}^2/Q^2) \right]$  [30, 31]. Red line (the example with additional mild power corrections):  $\phi_\pi(x) = \phi_{cz}(x)$ ,  $\Phi \simeq \sqrt{2}f_\pi \left[ 1.18 - (1.5 \text{ GeV}^2/Q^2) - (1.2 \text{ GeV}^2/Q^2)^2 \right]$ . Experiment: [20, 21, 23, 24].

1) A number of papers with predictions for  $F_{\gamma\pi}(Q^2)$  has been published, based on the model pion wave function  $\phi_\pi^{\text{BMS}}(x)$  (BMS=Bakulev-Mikhailov-Stefanis) obtained from the “improved QCD sum rules” with non-local condensates (see the last paper [25] and references therein). This approach has been criticized in [13], as it is based on arbitrary strong dynamical assumptions which, as was shown in [13], don’t pass the direct QCD check. Moreover, within this approach, one has to introduce a number of arbitrary model functions for various non-local vacuum condensates (see e.g. [26]) and, in general, the results for  $\phi_\pi(x)$  depend heavily on the model forms chosen for these functions (compare e.g. the results for  $\phi_\pi(x)$  from [27] and [26]). Finally, the model pion wave function  $\phi_\pi^{\text{BMS}}(x, \mu)$  obtained within this approach predicted the value of  $F_{\gamma\pi}(Q^2)$  only slightly above those for the asymptotic wave function  $\phi_\pi(x) = \phi_{\text{asy}}(x)$ , see [25], and well below the recent BABAR data [23, 24].

Besides, it is claimed in [25] that the data [20, 21, 23, 24] are incompatible with  $\phi_\pi(x, \mu) = \phi_{cz}(x, \mu)$  (and are even in contradiction with the QCD factorization for any pion wave function with the end point behavior  $\sim x(1-x)$  at  $x \rightarrow 0, 1$ ). As it is seen from Fig.9 (red curve), this is not so.

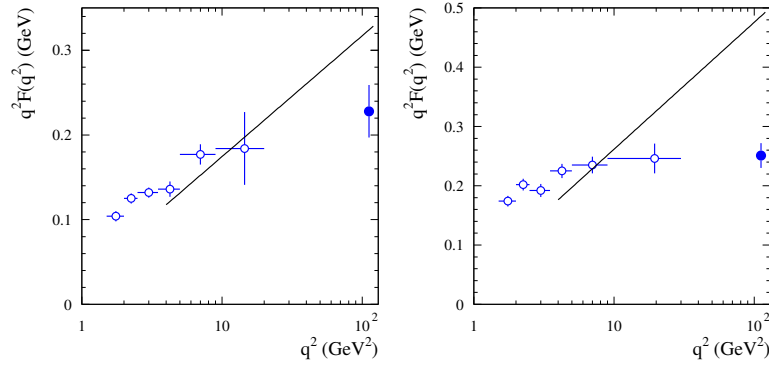


Fig. 10. Full points:  $|q^2 F_{\gamma\eta}(q^2)|$  (left) and  $|q^2 F_{\gamma\eta'}(q^2)|$  (right) transition form factors at  $q^2 = 112 \text{ GeV}^2$  [22]:  $|q^2 F_{\gamma\eta}(q^2)| = (0.229 \pm 0.030 \pm 0.008) \text{ GeV}$ ,  $|q^2 F_{\gamma\eta'}(q^2)| = (0.251 \pm 0.019 \pm 0.008) \text{ GeV}$ . White points: previous CLEO data at  $2 \text{ GeV}^2 < (Q^2 = -q^2) < 20 \text{ GeV}^2$  [21]. Black lines: the form factors  $|q^2 F_{\gamma\eta}(q^2)|, |q^2 F_{\gamma\eta'}(q^2)|$  for the flat pseudoscalar wave function  $\phi_P(x) \simeq 1$ .

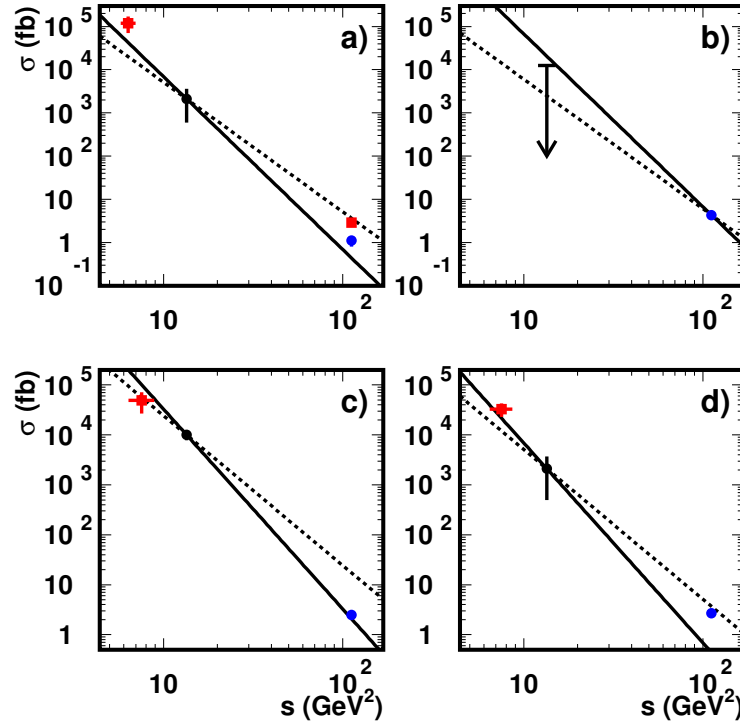


Fig. 11. Solid lines correspond to  $1/s^4$  dependence and dashed ones represent  $1/s^3$ . (a)  $\sigma(e^+e^- \rightarrow \phi\eta)$ ; (b)  $\sigma(e^+e^- \rightarrow \phi\eta')$ ; (c)  $\sigma(e^+e^- \rightarrow \rho\eta)$ ; (d)  $\sigma(e^+e^- \rightarrow \rho\eta')$ . The measured cross sections: at  $\sqrt{s} \simeq 2.5, 2.75 \text{ GeV}$  by BABAR [33], at  $\sqrt{s} = 3.67 \text{ GeV}$  by CLEO [34], at  $\sqrt{s} = 10.58 \text{ GeV}$  by BABAR [35] and Belle [36] for various processes. BABAR measurements are represented by squares. QCD predictions:  $\sigma(e^+e^- \rightarrow \text{VP}) \sim 1/s^4$  [1] (see (1),  $|\lambda_V| = 1$  in this case) up to a possible additional logarithmically growing factor [6], for the pseudoscalar wave function  $\phi_P(x)$  with the suppressed end point behavior, like  $\sim x(1-x)$  at  $x \rightarrow 0, 1$ .  $\sigma(e^+e^- \rightarrow \text{VP}) \sim 1/s^2$  for the flat pseudoscalar wave function  $\phi_P(x) \sim 1$ . The form factors  $\gamma^* \rightarrow \text{VP}$  are highly sensitive to the end point behavior of the leading twist pseudoscalar wave function  $\phi_P(x)$ , as they contain the factor  $I \sim \int_{\delta}^1 dx \phi_P(x)/x^2$ ,  $\delta = O(\mu_0^2/Q^2)$  [6]. So,  $I \sim \ln(Q^2/\mu_0^2)$  for  $\phi_P(x) \sim x(1-x)$ , while it will be parametrically larger at  $\phi_P(x) \sim 1$ :  $I \sim (Q^2/\mu_0^2)$ . The data are in a reasonable agreement (with a logarithmic accuracy) with the  $\sigma \sim 1/s^4$  dependence corresponding the end point behavior  $\phi_P(x) \sim x(1-x)$ , and are in contradiction with the behavior  $\sigma \sim 1/s^2$ , corresponding to  $\phi_P(x) \sim 1$  at  $x \rightarrow 0, 1$ .

Table 2. The values of form factors  $F_{\gamma P}(q^2)$  at  $q^2 = 112 \text{ GeV}^2$  for various meson wave functions.

wave functions	$ q^2 F_{\gamma^* \pi}(q^2) $	$ q^2 F_{\gamma^* \eta}(q^2) $	$ q^2 F_{\gamma^* \eta'}(q^2) $	Ref.
$\phi_n(x) \simeq \phi_s(x) \simeq \phi_{\text{asy}}(x) = 6x(1-x)$	0.14	0.13	0.21	
$\phi_n(x) \simeq \phi_s(x) \simeq \phi_{\text{cz}}(x)$	0.22	0.21	0.33	
$\phi_n(x) \simeq \phi_{\text{cz}}(x); \phi_s(x) \simeq \phi_{\text{asy}}(x)$	0.22	0.24	0.29	
$\phi_n(x) \simeq \phi_s(x) \simeq 1$	0.33	0.31	0.49	
experiment	–	$0.23 \pm 0.03$	$0.25 \pm 0.02$	[22]

After the new BABAR data on  $F_{\gamma\pi}(Q^2)$  [23] appeared, it was proposed in [28] that the large value of  $Q^2 F_{\gamma\pi}(Q^2)$  is due to the flat pion wave function,  $\phi_\pi(x, \mu) \simeq 1$ , as  $Q^2 F_{\gamma\pi}(Q^2)$  grows  $\sim \ln(Q^2/\mu_0^2)$  in this case and, taking  $\mu_0 \simeq m_\rho$  by hand, such a behavior fits well then these BABAR data. But in this case, because the wave functions of  $|\pi\rangle, |n\rangle$  and  $|s\rangle$  are qualitatively similar, see (7-8), the form factors  $q^2 F_{\gamma\eta}(q^2)$  and  $q^2 F_{\gamma\eta'}(q^2)$  will also grow the same way,  $\sim \ln(q^2/m_\rho^2)$  at  $q^2 \gg 1 \text{ GeV}^2$ . These two form factors have been measured recently by the BABAR Collaboration [22] at  $q^2 = 112 \text{ GeV}^2$ . It is seen from the Fig. 10 and Table 2 that with  $\phi_n(x) \sim \phi_s(x) \simeq 1$  these two form factors will be too large. Besides, such flat wave functions will contradict the data on  $\sigma(e^+e^- \rightarrow VP)$ , see Fig. 11.

## 5 Conclusions on the form factors $F_{\gamma P}(Q^2)$ , $P = \{\pi^0, \eta, \eta'\}$ and the leading twist wave functions $\phi_P(x)$ of pseudoscalar mesons

The flat leading twist pseudoscalar wave function

$\phi_P(x) \simeq 1$ :

a) predicts the form factors  $F_{\gamma\eta}(q^2)$  and  $F_{\gamma\eta'}(q^2)$  at  $q^2 = 112 \text{ GeV}^2$  considerably larger than the BABAR results;

b) predicts the parametrical behavior of cross sections  $\sigma(e^+e^- \rightarrow PV)$  at large  $s$  as:  $\sigma(e^+e^- \rightarrow PV) \sim 1/s^2$ , in contradiction with the data  $\sigma(e^+e^- \rightarrow PV) \sim 1/s^4$  in the interval  $\sim 8 \text{ GeV}^2 < s < 112 \text{ GeV}^2$ .

The asymptotic leading twist pion wave function  $\phi_\pi(x) \simeq 6x(1-x)$ :

a) predicts the form factors  $F_{\gamma\pi^0}(Q^2), F_{\gamma\eta}(Q^2)$  considerably smaller than data;

b) predicts branchings of charmonium decays:  $^3P_0, ^3P_2 \rightarrow \pi^+\pi^-, K^+K^-$ , the pion and kaon electromagnetic form factors  $F_{\pi, K}(q^2)$  at  $q^2 = 10-15 \text{ GeV}^2$  much smaller than data, etc.

The CZ leading twist pion wave function  $\phi_\pi^{\text{cz}}(x, \mu_0 \sim 1 \text{ GeV}) = 30x(1-x)(2x-1)^2$ : leads to predictions which, it seems, are not in contradiction with all data available.

*I am grateful to V.P. Druzhinin for explaining me details of various experimental results. This work is supported in part by the RFBR grant 07-02-00361-a.*



## References

- 1 Chernyak V L, Zhitnitsky A R. JETP Lett., 1977, **25**: 510
- 2 Chernyak V L, Serbo V G, Zhitnitsky A R. JETP Lett., 1977, **26**: 594
- 3 Chernyak V L, Zhitnitsky A R. Sov. J. Nucl. Phys., 1980, **31**: 544; Chernyak V L, Serbo V G, Zhitnitsky A R. Sov. J. Nucl. Phys., **31**: 552
- 4 Efremov A V, Radyushkin A V. Phys. Lett. B, 1980, **94**: 245; Teor. i Mathem. Fiz., 1980, **42**: 147
- 5 Lepage G P, Brodsky S J. Phys. Rev. D, 1980, **22**: 2157
- 6 Chernyak V L, Zhitnitsky A R. Phys. Rep., 1984, **112**: 173–318
- 7 Brodsky S J, Lepage G P. Phys. Rev. D, 1981, **24**: 1808
- 8 Benayoun M, Chernyak V L. Nucl. Phys. B, 1990, **329**: 285
- 9 Duplancic G, Nizic B. Phys. Rev. Lett., 2006, **97**: 142003
- 10 Chernyak V L, Zhitnitsky A R. Nucl. Phys. B, 1982, **201**: 492
- 11 Diehl M, Kroll P, Vogt C. Phys. Lett. B, 2002, **532**: 99; hep-ph/0112274
- 12 Chernyak V L. Phys. Lett. B, 2006, **640**: 246; hep-ph/0605072
- 13 Chernyak V L. Nucl. Phys. (Proc. Suppl.), 2006, **162**: 161; hep-ph/0605327
- 14 Nakazawa H et al (Belle collaboration). Phys. Lett. B, 2005, **615**: 39; hep-ex/0412058
- 15 Chen W T et al (Belle collaboration). Phys. Lett. B, 2007, **B651**: 15; hep-ex/0609042
- 16 Uehara S et al (Belle collaboration). Phys. Rev. D, 2008, **78**: 052004; arXiv: 0805.3387 [hep-ex]; 0810.0655 [hep-ex]
- 17 Uehara S et al (Belle collaboration). arXiv:0906.1464 [hep-ex]
- 18 Chernyak V L. Unpublished. 1976
- 19 Feldmann T, Kroll P, Stech B. Phys. Rev. D, 1998, **58**: 114006
- 20 Behrend H J et al (CELLO collaboration). Z. Phys. C, 1991, **49**: 401
- 21 Savinov V et al (CLEO collaboration). Phys. Rev. D, 1998, **57**: 33
- 22 Druzhinin V P et al (BABAR collaboration). Phys. Rev. D, 2006, **74**: 012002; hep-ex/0605018
- 23 Druzhinin V P et al (BABAR collaboration). Phys. Rev. D, 2009, **80**: 052002; arXiv: 0905.4778 [hep-ex]
- 24 Druzhinin V P. arXiv:0909.3148 [hep-ex]
- 25 Mikhailov S V, Stefanis N G. arXiv:0910.3498 [hep-ph]
- 26 Bakulev A P, Pimikov A P. Acta Phys. Polon. B, 2006, **37**: 3627; hep-ph/0608288
- 27 Radyushkin A V. Talk given at the Workshop “Continuous Advances in QCD”. University of Minnesota, Minneapolis, Feb. 18-20, 1994. In: Proc. “Continuous advances in QCD”, pp. 238-248; Preprint CEBAF-TH-94-13; hep-ph/9406237
- 28 Radyushkin A V. arXiv:0906.0323 [hep-ph]
- 29 Gosdzinsky P, Kivel N. Nucl. Phys. B, 1998, **521**: 274
- 30 Melic B, Muller D, Passek-Kumericki K. Phys. Rev. D, 2003, **68**: 014013
- 31 Khodjamirian A. Eur. Phys. J. C, 1998, **6**: 33; hep-ph/9712451
- 32 Braun V M, Filyanov I B. Z. Phys., 1990, **48**: 239
- 33 Aubert B et al (BABAR collaboration). Phys. Rev. D, 2007, **76**: 092005
- 34 Adams G S et al (CLEO collaboration). Phys. Rev. D, 2006, **73**: 012002
- 35 Aubert B et al (BABAR collaboration). Phys. Rev. D, 2006, **74**: 111103
- 36 Belous K et al (Belle collaboration). Phys. Lett. B, 2009, **681**: 400; arXiv: 0906.4214